Macromolecular Bioscience

Washless Method Enables Multilayer Coating of an Aggregation Prone Nanoparticulate Drug Delivery System with Enhanced Yields, Colloidal Stability and Scalability

--Manuscript Draft--

Manuscript Number:	mabi.201600535R1
Full Title:	Washless Method Enables Multilayer Coating of an Aggregation Prone Nanoparticulate Drug Delivery System with Enhanced Yields, Colloidal Stability and Scalability
Article Type:	Full Paper
Section/Category:	
Keywords:	Nanoparticle, liposomes, layer by layer self-assembled coating, polyelectrolyte multilayer films, aggregation
Corresponding Author:	Maryam Tabrizian McGill University Montreal, CANADA
Corresponding Author Secondary Information:	
Corresponding Author's Institution:	McGill University
Corresponding Author's Secondary Institution:	
First Author:	Lamees Nayef
First Author Secondary Information:	
Order of Authors:	Lamees Nayef
	Rafael Castiello
	Maryam Tabrizian
Order of Authors Secondary Information:	
Abstract:	Aggregation is frequently encountered during coating nanoparticles, especially when the core is not solid and the coating polyelectrolytes are weak. Here, the coating of a nanoliposome with two weak polyelectrolytes, alginate and chitosan, is investigated. First, Quartz Crystal Microbalance with Dissipation, Atomic Force Microscopy, Scanning Electron Microscopy, and Energy Dispersive Spectroscopy analyses confirm the feasibility of firm adsorption of up to 16 layers of weak polyelectrolytes to the liposomal surface. Titrations are then performed to identify the lowest amounts of polyelectrolytes required to make 8 saturated coating layers using the washless method. Significantly improved yields and reproducibility (almost 100%) are achieved, in addition to control over layer thickness. Attenuated Total Reflectance Fourier Transform Infrared Spectroscopy studies confirm the success of layering. This is special since scientists always attempt to reduce nanoparticle aggregation by substituting the soft core, using one strong polyelectrolyte, or contending with lower yields or numbers of coating layers.
Additional Information:	
Question	**Response**
Please submit a plain text version of your cover letter here. Please note, if you are submitting a revision of your manuscript, there is an opportunity for you to provide your responses to the reviewers later; please do not add them to the cover letter.	Dear Dr. Pfisterer, Please consider our attached manuscript, entitled “Washless Method Enables Multilayer Coating of an Aggregation Prone Nanoparticulate Drug Delivery System with Enhanced Yields, Colloidal Stability and Scalability” by Lamees Nayef, Rafael Castiello and Maryam Tabrizian for publishing in Macromolecular Bioscience. It is a research article discussing the multilayer coating of a challenging aggregation prone nanoparticulate drug delivery system. The system’s a soft core (liposome) and weak coating polyelectrolytes (alginate and chitosan), are a combination known by scientists to produce the lowest colloidal stability and hence mostly avoided.

	Here we report the successful assembly of 8 saturated coating layers on a soft liposomal core and using weak coating polyelectrolytes only. Applying the washless method along with detailed titrations led to significantly enhanced reproducibility and yields in comparison to prior attempts of coating by the authors. The achievement is special because it opens doors to experimentation with more nanoparticulate drug delivery systems and may increase the chances of large scale production for good candidates. Thank you, Maryam Tabrizian

DOI: 10.1002/marc.((insert number)) ((or ppap., mabi., macp., mame., mren., mats.))

Full Paper

Washless Method Enables Multilayer Coating of an Aggregation Prone Nanoparticulate Drug Delivery System with Enhanced Yields, Colloidal Stability and Scalability[a]

Lamees Nayef, Rafael Castiello, Maryam Tabrizian*

_____

Ms. Lamees Nayef., Mr. Rafael Castiello, Dr. Maryam Tabrizian
740-ave. Dr. Penfield, Room 4300, Montréal, QC H3A 0G1, Canada
E-mail: lamees.nayef@mail.mcgill.ca, francisco.castielloflores@mail.mcgill.ca, maryam.tabrizian@mcgill.ca
Dr. M. Tabrizian
3775-rue University, Room 313/308B, Montréal, QC H3A 2B4, Canada

_____

Aggregation is frequently encountered during coating nanoparticles, especially when the core is not solid and the coating polyelectrolytes are weak. Here, the coating of a nanoliposome with two weak polyelectrolytes, alginate and chitosan, is investigated. First, Quartz Crystal Microbalance with Dissipation, Atomic Force Microscopy, Scanning Electron Microscopy, and Energy Dispersive Spectroscopy analyses confirm the feasibility of firm adsorption of up to 16 layers of weak polyelectrolytes to the liposomal surface. Titrations are then performed to identify the lowest amounts of polyelectrolytes required to make 8 saturated coating layers using the washless method. Significantly improved yields and reproducibility (almost 100%) are achieved, in addition to control over layer thickness. Attenuated Total Reflectance Fourier Transform Infrared Spectroscopy studies confirm the success of layering. This is special since scientists always attempt to reduce nanoparticle aggregation by substituting the soft core, using one strong polyelectrolyte, or contending with lower yields or numbers of coating layers.

[a] **Supporting Information** is available online from the Wiley Online Library or from author.

Washless method titrations allow coating aggregation- prone liposome core nanoparticle with 8 layers of polyelectrolyte with higher yields and reproducibility promising greater success in investigating a broader range of multilayer coated nanoparticles for applications like drug delivery.

L. Nayef, R. Castiello, M. Tabrizian*

Washless Method Enables Multilayer Coating of an Aggregation Prone Nanoparticulate Drug Delivery System with Enhanced Yields, Colloidal Stability and Scalability

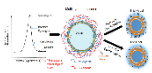

1. Introduction

Nanoliposomes are a very interesting class of nanoparticulate drug delivery systems that have been used for a variety of medical applications, ranging from vaccine delivery to fighting infection and eradicating tumours.[1, 2] Although disagreements exist in literature over the size of nanoparticles, drug delivery research often refers to particles less than 1000 nm as "nano", unlike material science research that defines them as particles less than 100 nm.[3-8] The size of nanoparticles is a critical point of discussion because of its responsibility for the special behaviors they exhibit. The small size of liposomes, for example, provides them with a special resemblance to biological structures in size allowing for easier escape from detection by the immune system.[9]

Many liposomal formulations have already been approved for use in humans by the FDA.[10, 11] However, despite their high level of biocompatibility, desirable control over their drug release kinetics has not yet been achieved.

Research over control of drug release kinetics from liposomes have centered over changing the bilayer constituents to influence the fluidity of their membranes.[12] Despite having success with hydrophilic drugs, this method had limited success with hydrophobic drugs packed into the membrane.[12, 13] The authors investigated coating the liposomes with multilayers of oppositely charged PE polymers using LbL self-assembly of multilayered films a few tenths of a nanometer.[14] The method is appealing because it allows modulating release rate for both hydrophobic and hydrophilic drugs, by simply adjusting the number of layers.[15] Self-assembly is more attractive than other methods like spin coating, thermal deposition and solution casting because of the fine control it offers over coat thickness and surface charge.[16] In addition, its simplicity, requirement of no sophisticated equipment and ability to coat almost any surface or shape makes LbL technique viable for large scale production by industry.[17]

While the LbL self-assembly coating of macro and micro templates was very successful, applying this method on nanoparticles with sizes less than 1000 nm has faced greater

challenges.[18-20] The challenges are due to a phenomena called "correlated adsorption" in which PE polymers adsorb, creating a polymer decorated nanoparticle rather than a fully coated nanoparticle.[21] This occurs because the repulsive forces between the adsorbed polymers cause them to lie slightly further apart from each other causing incomplete coverage of the nanoparticle surface with the PE.[22] The uneven covering decreases the colloidal stability of the nanoparticles, leading to rapid and easy aggregation unless conditions are perfectly controlled.[22, 23]

The most frequently used technique to overcome this limitation is incubating the nanoparticles with an excess amount of PE to ensure maximum coverage and maximize colloidal strength.[24] However, the method known as the method of excesses, requires the use of a high energy separation device like an ultracentrifuge to separate excess PE from the nanoparticles.[25] The separation is necessary to add the next layer of oppositely charged PE, which otherwise will associate with unbound excess of the previous PE. The high energy step causes the nanoparticles to aggregate, as even when excess PEs are used full coatings cannot be achieved, and colloidal strength is relatively poor.[21, 26] The result is the loss of nanoparticles with each coating step leading to very low yields as the number of layers increases, and decreasing the repeatability of the procedure.[27] The method has been used mostly with magnetic core nanoparticles as those can be separated from excess PEs using magnets.[28, 29] It has also been used with metallic cores which have a high density hence can be separated with lower gravity centrifugation without significant aggregation.[18, 19, 30-33] However, even with metal cores, aggregation losses have been reported specially at higher coat numbers.[31, 33] Attempts to coat soft core nanoparticles like liposomes using this method are fewer, and try to circumvent this problem by having fewer coats, and using ultrafiltration-centrifugation to remove excess PEs.[34, 35] However, losses can occur with this method as well due to coated liposomes sticking in aggregated form to the ultrafiltration membrane preventing their full recovery [unpublished data by the authors].

A less frequently and more recently developed method called the washless method uses the lowest amount of polymer needed to build up a saturated coating eliminating the need for separation steps.[25, 36, 37] Despite the presence of several papers that tried using few concentrations of PEs and the choice of the concentration that gives the best colloidal stability,[38-40] this method ensures reaching the maximum colloidal strength possible by allowing each coating layer to reach saturation through the use of a detailed titration curve.[21, 25] The titration curves allow determining the amount of PE that produces a saturated coating and leaves negligible excesses.[25] The method is simpler, uses less sophisticated equipment and has a lower energy consumption. It also maximizes the yield and provides greater flexibility with the number of coating layers that can be assembled.[41] In addition, the method is especially desirable for soft core nanoparticles coated with weak PEs, known to produce the weakest colloidal stability and most aggregation.[28] In addition, thickness of deposited layers can be easily tuned using dilutions.[42]

In this paper, nanoliposomes of approximately 200 nm diameter are coated with alternating layers of alginate and chitosan known as weak PEs **(Figure 1)**. The combination of a liposomal core, alginate and chitosan PE coats is highly desirable for the intended use of the nanoparticles in drug delivery because all constituents have been approved by the FDA for some uses in humans.[43-45]

The coating was attempted previously by Haider et al. using the excess method, and the capacity of layer addition to allow controlled drug delivery confirmed.[46, 47] However, the soft core and weak PEs made the nanoparticles highly prone to aggregation.[28, 31, 48, 49] This caused most nanoparticles to be lost totally after the addition of 4 layers. The achievement of 6 coating layers was possible only twice by the author. However, in both attempts most nanoparticles were lost to aggregation during centrifugation cycles, and less than 5% remained un-aggregated after the addition of 6 layers. Therefore, the washless method is

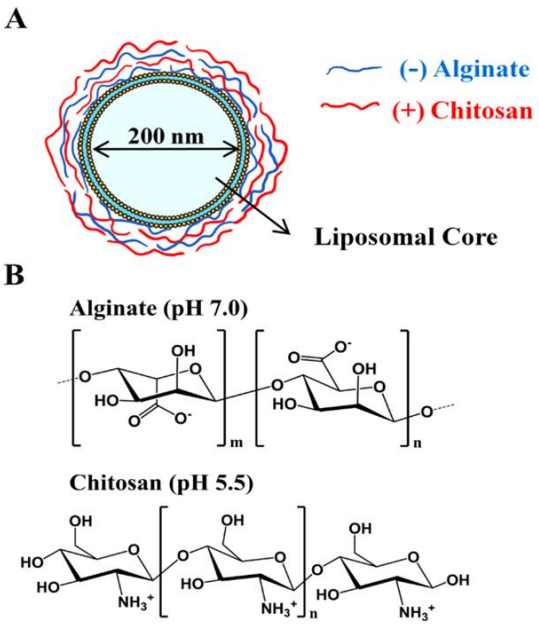

*Figure 1.*A) Diagram of the nanoliposomal drug delivery system with multilayer coatings of negatively charged alginate and positively charged chitosan assembled by LbL technique. B) Chemical structure and charge of both PEs in the solutions used for their LbL-assembly

attempted as an alternative procedure. The feasibility of LbL assembly of chitosan and alginate on the liposomal surface is investigated first in a 2D model using a combination of QCM, AFM, SEM and EDS analyses. This was performed to ensure that the low yields and repeatability achieved through the excess method are not due to the inability of large numbers of the weak PEs to adsorb firmly to the liposomal surface. Titrations were then used to determine the exact amount of PEs needed to create a saturated coating layer for the nanoliposomes in solution through the washless method. Finally, ATR-FTIR was used to confirm the accuracy of the titrations through monitoring the characteristic peaks corresponding to each PE in the supernatant for each layer.

2. Experimental Section

2.1. Materials

Liposomes were made from 1, 2-dihexadecanoyl-sn-glycero-3-phosphocholine (DPPC) purchased from Cordon Pharma (Switzerland), dimethyldioctadecylammonium bromide (DDAB) from Sigma-Aldrich (USA) and cholesterol from Sigma-Aldrich (USA). Chloroform

(99.9%) and methanol (99.9%) were purchased from Fischer Scientific (USA). Polyelectrolyte solutions were prepared using Alginic acid (12 kDa, viscosity $2.5x10^{-1}$ Pa.s, 2% (25°C), Chitosan (91 kDa, deacetylation 83.2%, viscosity $2x10^{-2}$ Pa.s), acetic acid (99.9%) and sodium hydroxide from Sigma Aldrich (USA).

2.2. Methods

2.2.1. Preparation of liposomes

Liposomes were prepared by dissolving 100 mg of DPPC, 26.3 mg of Cholesterol and 5.15 mg of DDAB (4 mol% of lipids used) in 5 ml of 4: 1 chloroform: methanol (v/v). The mixture was introduced in a round bottom flask and attached to a rotoevaporator to allow the evaporation of organic solvents. A vacuum pressure of 50 cmHg and a heated water bed (43°C) were used as evaporation aids. The dry thin lipid film was hydrated with 5 ml of Milli-Q water at the same temperature. The liposomal mixture was extruded through 200 nm, 19 mm polycarbonate filters (Whatman, USA) using a mini extruder (Avanti Polar Lipids, USA). The hydrodynamic diameter and the zeta potential of the extruded liposomes were checked using a ZetaPALS instrument with a particle sizing option (Brookhaven Instruments, USA).

2.2.2. Preparation of PE solutions

A stock solution of 1 mg/ml alginate was prepared and its pH adjusted to 7.0 using 1M sodium hydroxide solution. A stock solution of 1 mg/ml chitosan was also prepared with chitosan dissolved in Milli-Q water with 1 v/v% acetic acid and the pH was adjusted to 5.5 using 1 M sodium hydroxide solution. Back titrations were not used as they increase the concentration of salts in the coating solutions.

2.2.3. Characterizing adsorption of PE multilayers on liposomes using QCM-D

QCM-D measurements were performed with a Q-Sense E4 unit (Q-Sense, Sweden) by simultaneously monitoring the changes in frequency (Δf) and energy dissipation factor (ΔD) after each layer deposition. The QCM-D crystal was excited to oscillate at its fundamental resonance frequency (f = 5 MHz) and odd overtones (ν = 3, 5, 7, etc.) by applying a radio-frequency voltage across the electrodes. For all experiments, QCM-D quartz sensors with a 100 nm gold layer (QSX 301) were used. All sensors were cleaned in UV/ozone (UV-ozone chamber Biofore Nanosciences, Inc.) for 10 minutes, then placed in a 5: 1: 1 solution of Milli-Q water, ammonia (25%) and hydrogen peroxide (30%) at approximately 75°C for 5 minutes. Finally, the sensors were treated again with UV/ozone for an additional 10 minutes. In order to confirm the adsorption of PE multilayers on the surface of 200 nm liposomes, 700 µl of 1 mg DPPC/ml liposomes were incubated on a cleaned gold QCM-D sensor for 8 minutes. Milli-Q water was flowed at 100 µl/min for 10 minutes to wash any weakly adsorbed liposomes. Alginate (1 mg/ml) or chitosan (1 mg/ml) aqueous solutions were then introduced at 100 µl/min for 15 minutes over adsorbed liposomes to build PE multilayers. Milli-Q water was flowed at 100 µl/min for 10 minutes in between layers to wash any excess PEs. The procedure was repeated to allow 4, 6 and 16 alternating layers of PEs to self-assemble over liposomes. This experiment was performed 3 times on different QCM-D sensors. Two additional QCM-D sensors were used as negative controls by omitting the initial liposome incubation step and exposing the sensor sequentially to 4 and 12 PE layers to verify whether buildup of PEs occurs over the bare gold surface.

2.2.4. Characterizing of Adsorption of PEMs using AFM

The topography of a clean gold QCM-D sensor, the negative controls (PEs with no liposomal core) and the various layer-coated liposomes were characterized by AFM using a Nanoscope III instrument (Digital Instruments, USA) and later analyzed using Nanoscope v 5.12r5 software. AFM images were obtained in tapping mode in air at room temperature with a silicon

probe with a nominal spring constant of 42 N/m and a nominal resonance frequency 330 kHz (model PPP-NCHR, NANOSENSORSTM). Depth histograms were acquired for 100 x 100 µm sections of the gold QCM-D sensor for all samples. The most frequently encountered height was taken as an indication of the average height of attached particles and used to verify the attachment of PE multilayers on liposomes.

For SEM and EDS analyses, the same procedure described above was applied to prepare liposomes and liposomes+ 6 and 16 layers of PEs on new QCM-D sensors. Immediately after the layering process ended on the QCM-D gold sensors, the sensors were dried under a stream of nitrogen and a 5 nm layer of Ti was deposited on them with a Leica Microsystems EM ACE600 High Resolution Coater. A control gold QCM-D sensor with only 16 layers of PEs was also assembled. The coating morphology was then characterized using a Field Emission Inspect F50 Scanning Electron Microscope (FE-SEM), equipped with an EDAX Octane Super 60 mm2 SDD and TEAM EDS analysis system and compared with bare liposomes.

2.2.5. Titrations to determine the optimal amounts of PEs needed for coating liposomes

The extruded liposomal mixture was diluted to 0.2 mg/ml with Milli-Q water. Increasing volumes of 1 mg/ml alginate solution were pipetted to polystyrene disposable cuvettes filled with a fixed volume (0.5 ml, corresponding to 0.1 mg DPPC) of the diluted liposomal mixture. The cuvettes were then incubated at room temperature for 20 minutes. The hydrodynamic diameter, PDI and zeta potential of resulting particles were then measured and plotted versus the amount of added PE to visualize the data. The lowest amount needed for making a saturated coating layer was taken as the first point after the peak in the diameter versus titrant curve, when adding more PE does not cause a significant decrease in hydrodynamic diameter and when the zeta potential is above 30 mV in magnitude. This process was repeated to find all minimum amounts needed for making stable eight layer coated nanoparticles. For example, a minimum amount of 1 mg/ml alginate solution needed to create a saturated stable first layer

coating for 0.5 mL of the diluted liposomes was found from titration curves to be 3 μL. Titrations for the second layer are performed by incubating 3 μL of 1 mg/ml alginate with 0.5 mL of the diluted liposomes for 20 minutes in different cuvettes. Different and increasing volumes of 1 mg/ml chitosan solutions are then incubated for an additional 20 minutes and the hydrodynamic diameter, zeta potential and PDI of the resulting nanoparticles in each cuvette recorded in titration curves showing the variation of each property against added chitosan solution volume. The changes that occur when 0-6 μL of chitosan solution are incubated were recorded, with measurements made every 0.1 μL in regions where the desired properties change most, and every 1 μL in regions where the properties change least. The minimum volume of chitosan needed to create a stable second layer is chosen from the second set of titration curves as described above, and the process is repeated for the subsequent layer. The incubation time for all layers was 20 minutes, except for layer three, where optimizations showed that a seven-minute incubation period gives the optimum results.

2.2.6. PE multilayers film thickness adjustment through dilutions

Dilutions were performed before deposition of layer 7 to investigate the ease of controlling the hydrodynamic diameter of the nanoparticle. An equal volume of milli-Q water was added to the 6-layer nanoparticle suspension to half its ionic concentration. New titration curves were plotted to find the lowest amounts of PEs needed to produce saturated coatings after the dilution. The titration curves were conducted as described in previous sections. The procedure was tested to limit the nanoparticle hydrodynamic diameter after layering to less than 500 nm.

2.2.7. PEs multilayer analysis using ATR-FTIR

A 1 mm×1 mm piece of glass substrate was cleaned using subsequent washing with soap, acetone, isopropanol and Milli-Q water. One droplet of 33.3 μl of each layered sample was then deposited on the substrate and allowed to dry at room temperature. This step was repeated 3

times to achieve a final deposited volume of approximately 100 µl for each sample. Similarly, a volume of 2 mL was taken after the addition of each PE layer and ultra-centrifuged at a speed of 50000 rpm (108,628xg), using a Beckman ultracentrifuge (rotor TLA-100.2) and deposited on a glass substrate. The speed of ultracentrifugation was chosen through optimizations so that it is only sufficient to pellet the bare liposomes. The substrates with the deposited samples were mounted on top of the Ge ATR crystal and pressed gently against its surface using a sample clamp incorporated to the instrument to achieve optimal contact between the surface of the sample and the crystal. FTIR spectra were then acquired in transmission mode with OPUS software version 7.2 at a spectral resolution of 4 cm^{-1} within a 4000–600 cm^{-1} range and averaging 128 scans per sample using a Bruker Tensor 27 spectrophotometer equipped with an ATR module, a MIR source and a MCT detector cooled with liquid nitrogen. Baseline correction and atmospheric compensation was performed to all spectra.

3. Results and Discussion

3.1. QCM-D and AFM data show adsorption of up to 16 layers of PEs

QCM studies were performed using excess PEs to ensure the ability of large numbers of layers of the relatively weak PEs to adsorb to the liposomal surface before more time consuming titrations are performed. Frequency of gold-surface quartz crystal, indeed decreased after allowing 1 mg (DPPC)/ml liposome suspension to settle on its surface **(Figure 2 A)**. The decrease remained even after the washing step showing that liposomes adsorbed firmly to the gold surface of the crystal.[50, 51] Frequency also decreased when 4, 6 and 16 layers of alternating PEs were allowed to flow over liposomes adsorbed to gold surface crystals as shown in **Figures 2 B-D**. Washing steps after each deposition increased frequency slightly, but never higher than frequencies prior to each layer deposition.

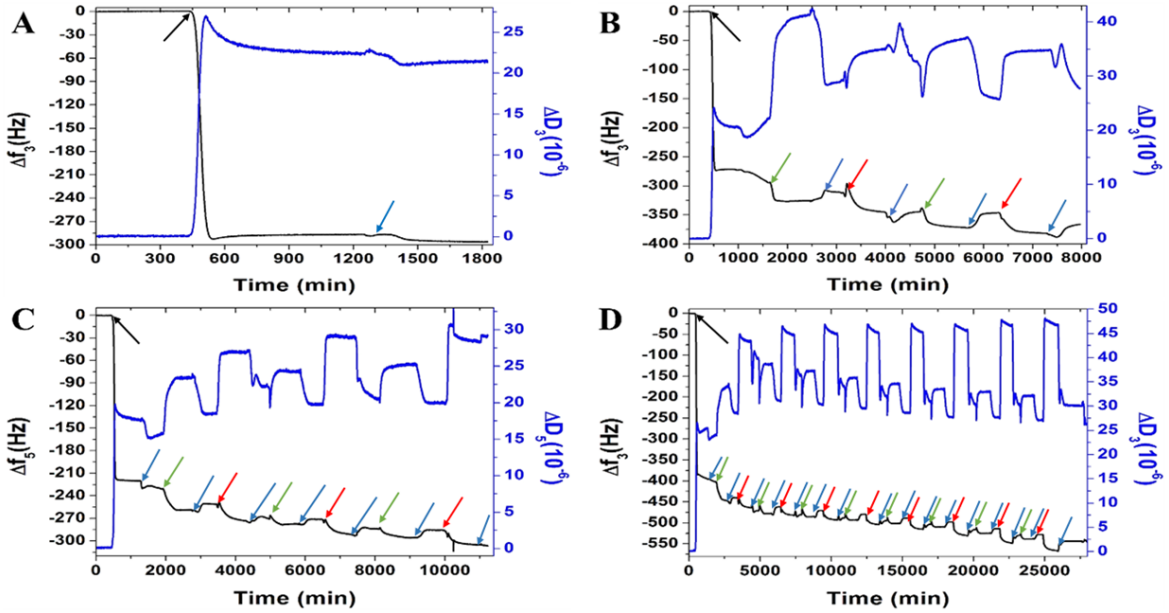

Figure 2. Frequency changes (black line) as recorded by QCM-D after the deposition of A) Liposomes only, B) Liposomes+ 4 layers of PE, C) Liposomes+ 6 Layers of PE and D) Liposomes+ 16 Layers of PE. Blue lines in each diagram represent the corresponding dissipation energy. Different colored arrows represent the time points of permission of different solutions: 1mg DPPC/ml liposomal solution(black), 1mg/ml alginate and chitosan solutions (green and red respectively) and Milli-Q water for washing (blue)

AFM studies used in conjugation with QCM-D for samples containing various numbers of layers up to 16 layers confirmed the PE adsorption on liposomes. Top and 3D profile AFM images of the quartz crystals' surfaces after depositions showed protrusions indicating the underneath adsorbed liposomes **(Figure 3 A to D)** as compared to AFM images of bare gold surface quartz crystals **(Figure 3 E)**. Depth histograms measuring heights of protrusions on each crystal over sample areas of size 100 µm x 100 µm are shown in Figure 1S in attached supplementary materials.

The average heights of protrusions, taken as the most frequently encountered protrusion heights in the histograms are summarized in the table in **Figure 3 F**. The average height increases slightly with the addition of 4 and 6 layers of PEs. However, after the addition of 16 layers, the increase in height became clearly distinguishable both in the 3-D profile AFM image **(Figure 3 D)** and average height measurements **(Figure 3 F)**. The increase in height further consolidated QCM-D finding that multilayer coating occurred on the liposomes.

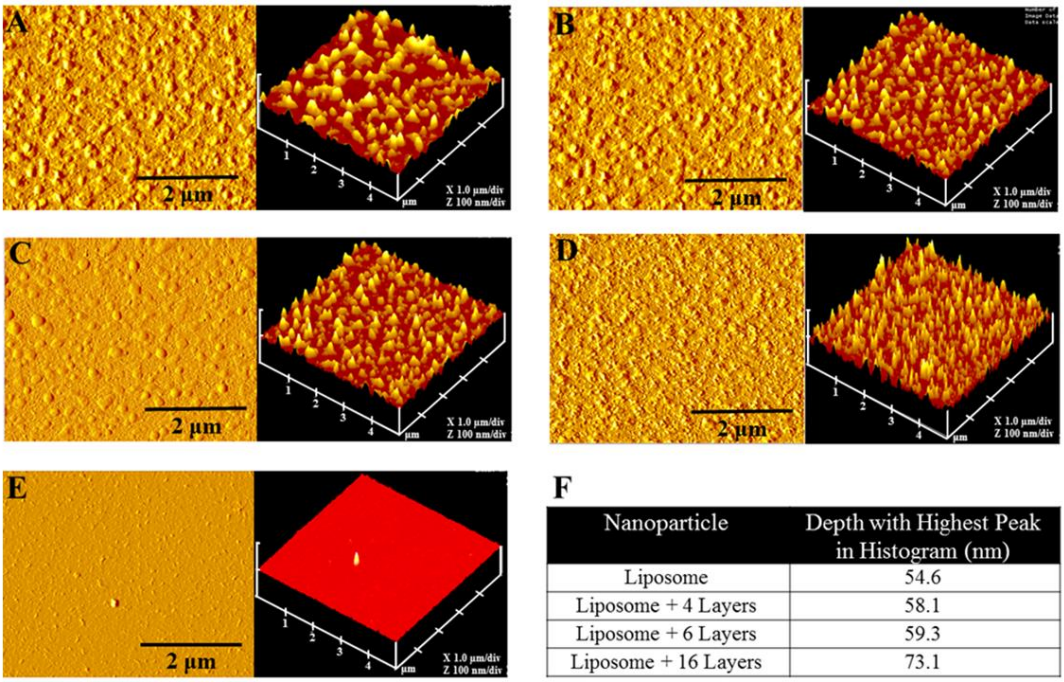

F

Nanoparticle	Depth with Highest Peak in Histogram (nm)
Liposome	54.6
Liposome + 4 Layers	58.1
Liposome + 6 Layers	59.3
Liposome + 16 Layers	73.1

Figure 3. 2-D and 3-D AFM images of gold QCM-D sensors for (A) liposomes deposited alone, (B) liposomes + 4 PE layers, (C) liposomes + 6 PE layers, (D) liposomes + 16 PE layers and (E) clean QCM-D sensor surface respectively. All images have the same height scale of 100 nm. F) Table showing average depth of peaks (within an area of 100 µm X 100 µm on each QCM-D sensor) obtained from AFM histograms presented in Figure 1S

Further analysis of negative controls revealed that the decreases noted in the frequency of the crystals after depositing the various layers on attached liposomes are not due to depositions on unoccupied gold surfaces between attached liposomes on the crystal. QCM-D measurements of frequency decreases after depositing 4 and 16 layers of PEs without prior attachments of liposomes to the gold surface showed that most of the PEs deposited are washed away in subsequent rinsing steps **(Figure 4 A and B)**. This leads to much lower depositions than witnessed when the same number of layers are deposited on liposomes. A 20 and 100 Hz decrease in frequency of the QCM-D sensor occurred when 4 and 16 layers of PEs are deposited on the surface of the QCM-D sensor for instance, in comparison with 87 and 140 Hz respectively for sensors with the same number of layers with liposomes adsorbed. Despite the availability of the entire gold surface for PEs to bind **(Figure 4 C)**, only these small random depositions are noticed **(Figures 4 E-F)**. Conversely, higher depositions occurred when

liposomes were attached even though the availability of very little exposed gold surface **(Figure 4 D)**. Chitosan and alginate showed a low binding capacity to the gold surface of the quartz crystal confirming that they adhered almost entirely on the liposomal surfaces.

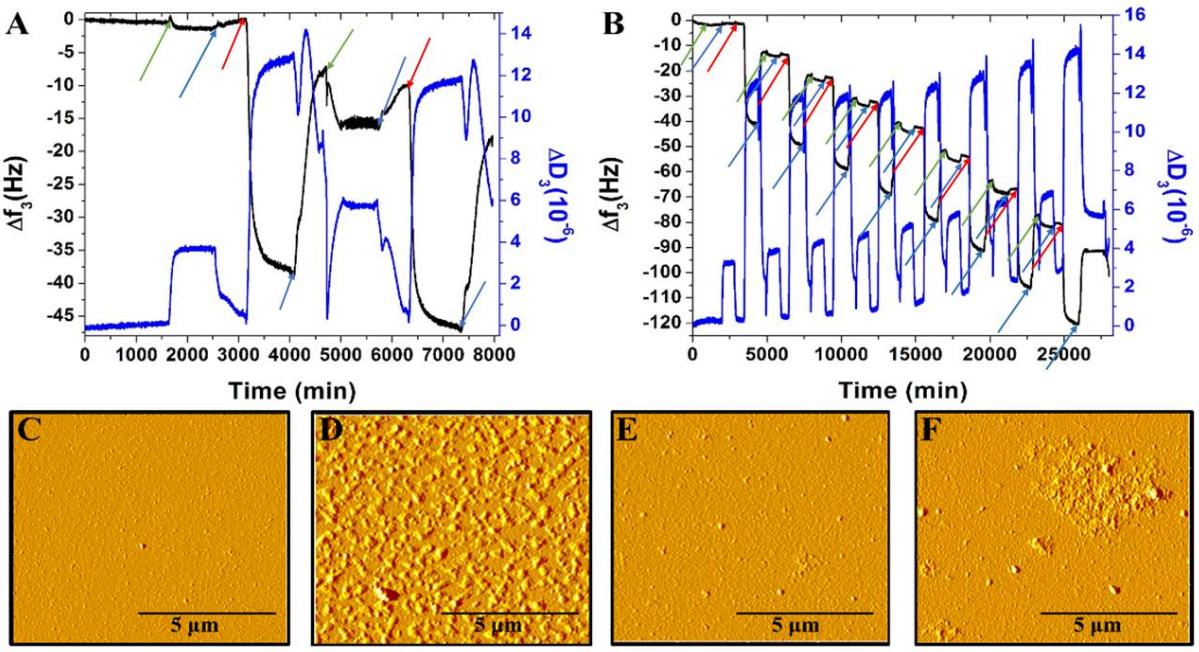

Figure 4. A) Frequency changes in QCM-D experiment (black line) for A) negative control showing the depositions after flowing 4 PE layers (no liposomes) and B) 16 layers of PE (no liposomes). Blue lines show the corresponding change in dissipation. Green and red arrows represent points of permission of 1mg/ml alginate and chitosan solutions respectively, while blue arrows represent points of permission of Milli-Q water for washing. C) 2D AFM image of a clean QCM-D sensor, D) QCM-D sensor with liposomes only, E) QCM-D sensor of negative control with 4 PE layers (no liposomes) F) QCM-D sensor of negative control with 16 PE layers (no liposomes).

3.2 SEM and EDS analysis confirm adsorption occurs at the surface of Liposomes

SEM images **(Figure 2S)** taken of layered liposomes attached to QCM-D sensors surfaces matched the AFM images, while the EDS analysis verified the successful coating of the nanoliposomes **(Figure 3S)**. This can be observed in the progression of the C: Au peak ratio on the EDS survey of the elements. For instance, on Figure 3S A which shows the surface of a clean QCM-D sensor, the C peak is very small compared to the Au peak. Once nanoliposomes are deposited on the QCM-D sensor surface **(Figure 3S B)** the C peak increases notably. Later the C: Au ratio also increases as 6 PE layers **(Figure 3S C)** and 16 PE layers **(Figure 3S D)** are deposited.

3.3. Titration curves enabled finding the optimal amount of PEs needed to form washless multilayered liposomes

The results obtained with QCM-D and AFM using the 2D model, confirming the adsorption of up to 16 layers of PEs on liposome, were employed to develop the protocol for coating the liposomes in free solution. The titration curves used to find the lowest amounts of alginate needed to make the first saturated layer are shown in **Figure 5**. The diameter of particles when small amounts of PEs were added to them, increased as shown in **Figure 5 A** until it reached a peak, then decreased to approximately the size of the original particle. Further addition of PEs did not cause significant decreases in diameter.

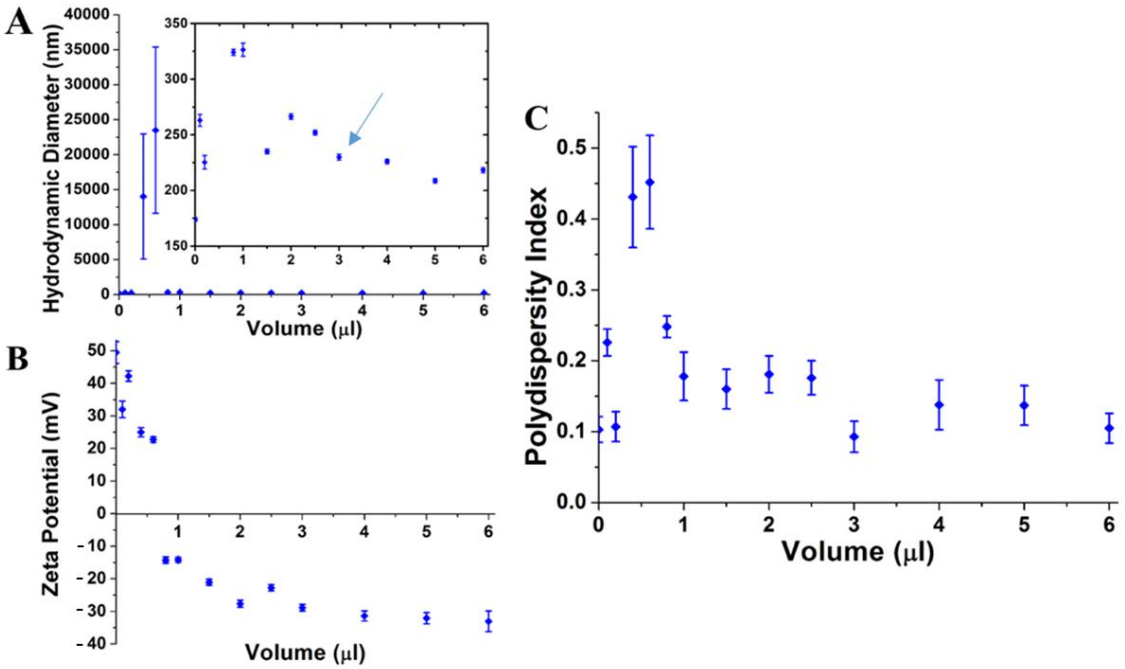

Figure 5. Titration curves used to find the optimal volume of a 1 mg/ml solution of alginate to form the first saturated coating layer over 0.5 ml of 0.2 mg/ml DPPC (0.1 mg DPPC) liposome solutions. A) Graph showing the variation in hydrodynamic diameter of the nanoparticles vs the volume of alginate solution added. The inset indicates the smaller diameters at a different scale for easier reading. Arrow shows the volume deduced from the curves to be the lowest needed to make a stable saturated first layer coating (first volume after the peak where no significant decreases in volume occurs and the zeta potential is above 30mV in magnitude). B) Variation of the zeta potential of the same nanoparticles vs the volume of alginate solution added. C) Variation of polydispersity of same nanoparticles as a function of added volume of alginate solution.

Meanwhile, the zeta potential of the particles **(Figure 5 B)** became more negative as more alginate was added. It reached a value of zero when the same volume of alginate that caused

the highest peak in diameter to occur was mixed. From this point onwards, the addition of alginate caused the zeta potential to keep increasing in negativity. The increase in negativity finally slowed down.

The switching of the zeta potential sign and its increase in negativity occurred at the same alginate volumes that caused the diameter of the particles to decrease from the peak. The PDI of the particles shown in **Figure 5 C**, reached a maximum at around the same volumes of alginate at which the peak in particle diameters, and the zero zeta potential value was attained.

The behaviour observed is consistent with the theory for coating colloids with oppositely charged PEs.[21, 52, 53] The increase in diameter occurs because increasing amounts of negatively charged alginate adhere to the positively charged liposomes decreasing their net charge. When the particle is neutralized, or the isoelectric point is reached, the zeta potential reaches zero, and there is zero repulsion between particles.[21] The particles are decorated with patches of negatively charged alginate, causing their surface charge at different locations to be heterogeneous.[54, 55] This triggers the particles to attract together and cluster forming larger particles representing the peak diameters that occur when the zeta potential reaches zero **(Figure 5 A)**. **Figure 5 C** shows that the PDI is highest at that point because aggregation causes many non-uniform sized clusters.

The decrease in diameter witnessed at adding more alginate occurs due to a phenomenon called overcharging, in which PEs arrange themselves onto the surface of the colloid and allow the neutral liposome to paradoxically attract more negatively charged alginate until saturation is reached.[17, 53, 56] At this point, extra alginate does not adhere and remain in solution.[55] The increase in negative net charge causes more repulsions between particles allowing smaller clusters to form. This explains the decrease in particle diameter observed after the zeta potential reverses **(Figure 5 A, B)**. When saturation occurs, diameter cannot decrease further since only single liposomes covered with one layer of alginate are present. When a maximum threshold

concentration, after the saturation point, is reached irreversible coagulation of PE and nanoparticles occurs.[17, 21, 55]

This phenomenon allowed us to identify the minimum amount of alginate needed to reach the saturation point when the diameter stops decreasing in the titration curves.[25] When that amount of alginate is added, no excess alginate remained in solution. At the saturation point the zeta potential was always ≥ 30 mV in magnitude, confirming the formation of a stable colloid.[57, 58] The PDI also reduced back to less than 0.3 showing a uniform distribution of nanoparticles, and confirming the disappearance of clusters.[59] A schematic titration graph illustrating the different zones and points discussed to coat a nanoparticle with an oppositely charged PE is presented in **Figure 6**. Irreversible coagulation due to reaching maximum salt concentration threshold is not shown since it is irrelevant to the current study.[17, 21, 55] Eight sets of titration curves were plotted for each layer added to find the optimal amounts of PE needed to coat the liposomes in free solution with 8 layers. **(Figures 4S-10S)**. These minimum amounts of PEs to form each saturated layer, are summarized in **Table 1 (columns 2-4)** with the resulting particle diameters and zeta potential.

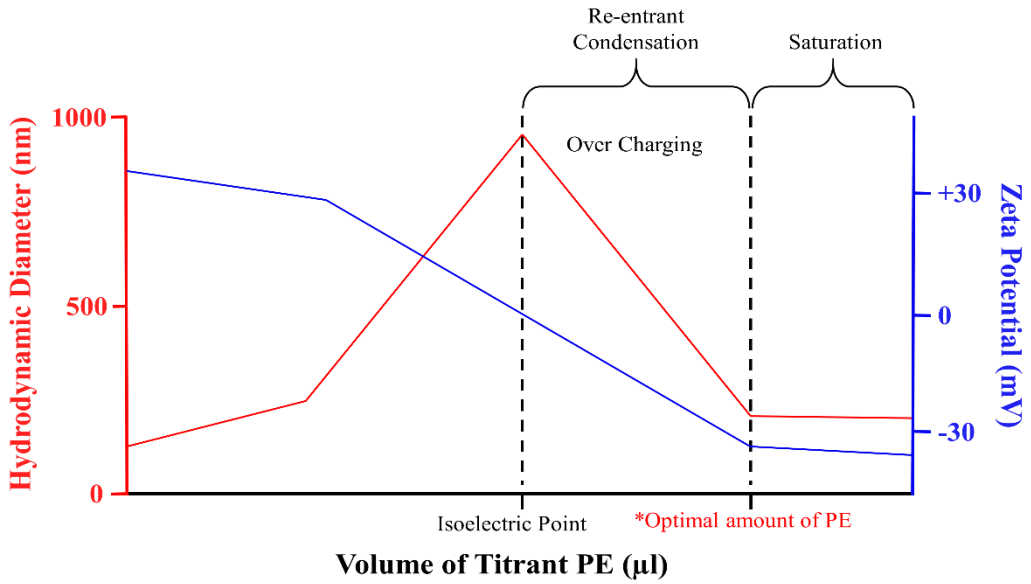

Figure 6. Diagram showing zones of re-entrant condensation, overcharging and saturation along with the isoelectric point and point taken as optimal amount of PE solution needed to create a single saturated coating layer. All zones and points labelled on the graph show the hypothetical

variation of hydrodynamic diameter (red) and zeta potential (blue) of positively charged nanoparticles coated by a negative PE.

Table 1. Optimal volumes of PE to produce each saturated coating layer for liposomes found from titration curves along with hydrodynamic diameters of the nanoparticles and zeta potential without (columns 2 to 4) and after the dilution (columns 5 to 6) to make layers 7 and 8 adjustments to reduce particle size. Odd numbered rows represent alginate layers while even numbered rows represent chitosan layers.

Layer No.	Volume of PE [µL]	Hydrodynamic Diameter [nm]	Zeta Potential [mV]	Volume of PE after Dilution [µL]	Hydrodynamic Diameter after Dilution [nm]	Zeta Potential [mV]
0	**0.0**	**174 ± 1.7**	**49.5 ± 3.4**	**-**	-	-
1	**3.0**	**229 ± 2.6**	**-28.8 ± 1.0**	**-**	-	-
2	**3.2**	**273 ± 3.4**	**58.8 ± 1.6**	**-**	-	-
3	**2.0**	**241 ± 1.8**	**-48.6 ± 1.6**	**-**	-	-
4	**28.0**	**182 ± 2.4**	**40.3 ± 3.4**	**-**	-	-
5	**37.0**	**372 ± 8.6**	**-60.0 ± 1.2**	**-**	-	-
6	**23.0**	**294 ± 5.0**	**42.6 ± 2.1**	**-**	-	-
7	**57.0**	**570 ± 17.1**	**-48.7 ± 0.7**	**47.7**	**361.8 ± 7.4**	**-44.6 ± 1.6**
8	**104.6**	**635 ± 15.2**	**33.0 ± 1.3**	**87.4**	**476 ± 17**	**34.94 ± 1.0**

3.4. Dilutions allow limiting the final size of 8 layer coated particles

Controlling the size of a nanoparticle delivery system is very important for its function. The addition of more than 6 layers of coating increased the size of the nanoparticles to greater than 500 nm which is reported not in the optimum size range for many biomedical application.[60, 61] The thickness of layers in LbL self-assembly of PEs on surfaces is known to be influenced during deposition by a variety of factors, namely PE type, deposition time, temperature, pH, ionic charge, and concentration.[17, 62, 63] Among these parameters, we investigated the effect of diluting ionic concentration during depositions as it was an easy process and a viable option for scale up. We found that the effect of salt on adsorption of PEs is concentration dependent.

Below a minimum threshold concentration, adsorption of PEs does not occur.[17, 42] Above that threshold, increasing salt concentrations increases the screening of PE charges allowing them to take a more coiled conformation.[64] An extended conformation occurs at low concentrations due to repulsions between the similarly charged units of the PEs.[42] When PEs are deposited in solutions with high ionic concentrations, they adhere to the nanoparticle in their coiled conformation making the layer thick as schemed in **Figure 7**.[17, 64] The coiled conformation adheres to the nanoparticles at fewer points allowing space for more PEs to attach and resulting in layers of increased thickness and mass.[62, 64]

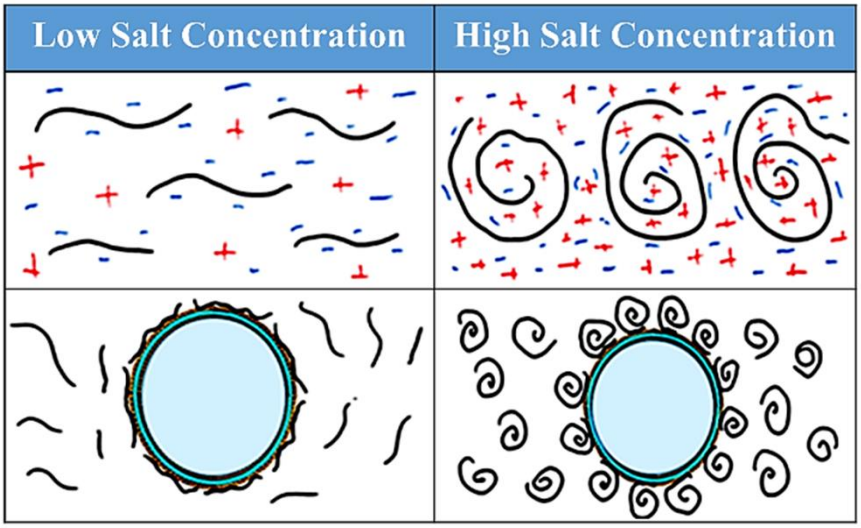

Figure 7. Schematic representation of the effect of salt concentration on the PE conformation and the corresponding effect on coat thickness when PE are used for coating. At low salt concentration the PE present a stretched conformation (left column). At high salt concentrations the PE present a coiled conformation (right column).

As the PE solutions added have large amounts of salts needed for keeping them buffered at constant pH, the accumulation are expected to be maximum towards the last layers. The large nanoparticle diameters obtained for layer 7 and 8 are due PE adsorbing in the globular conformation forming thicker and higher mass coats. The nanoparticle suspension was therefore diluted to half its ionic concentration after incubating the sixth PE layer. Using the new titration curves **(Figure 11S-12S)** to find the lowest amount of PEs to make saturated coating layers after dilution resulted in reducing the hydrodynamic diameter of the

nanoparticles **(Table 1, Columns 4 to 6)**. This is consistent with theory which predicts that thinner and lower mass saturated coats will be produced.

Fluctuations in nanoparticle size occur within each group (undiluted and diluted). The addition of an alginate layer almost always results in an increase in diameter, while the addition of chitosan resulting in some shrinkage **(Table 1)**. The fluctuations witnessed are due to a commonly noted phenomena concerned with excess uncompensated positive or negative charge in weak PE multilayer films called "the odd even effect" [65, 66]. The nanoparticle coated here appears to have uncompensated negative charges. When the last layer is negative (alginate), positive ions are attracted near the nanoparticle. This causes more positive ions to move towards the uncompensated charges in the PE multilayers [65]. Water follows into the multilayers to decrease the building osmotic pressure (due to increased salt ions). The entire multilayer coat swells. The opposite occurs when the last layer is positive (chitosan) [65, 66]. The swelling and shrinkage is most pronounced with weak PE: their weak association increases the chance of having uncompensated charges and the ability to uptake and expel large volumes of water [66-68].

3.5. FTIR analysis confirms the adsorption of the used amounts of PE during the LbL assembly

Figure 8 A shows the characteristic spectra for chitosan, alginate and liposomes. In the spectrum of chitosan, the broad band at 3265 cm^{-1} and 3180 cm^{-1} corresponded to the hydroxyl and amine groups respectively; the peak at 3000 cm^{-1} correspond to -OH stretching; the characteristic peaks of C=O and NH of the amide-II group at 1600 cm^{-1} and 1572 cm^{-1} respectively. It also indicate a strong band at 1410cm^{-1} that correspond to the CH_2-OH groups.[69, 70] As for alginate, the broad band between 3630-3230 cm^{-1} corresponds to the –OH stretching; the peak at 1610 cm^{-1} and 1410 cm^{-1} are characteristics of symmetric and asymmetric stretching of the COO- group, respectively. Additionally, the peak at 1033 cm^{-1} is associated with the C-O-C stretching mode attributed to its saccharide structure.[71, 72] For liposomes, the

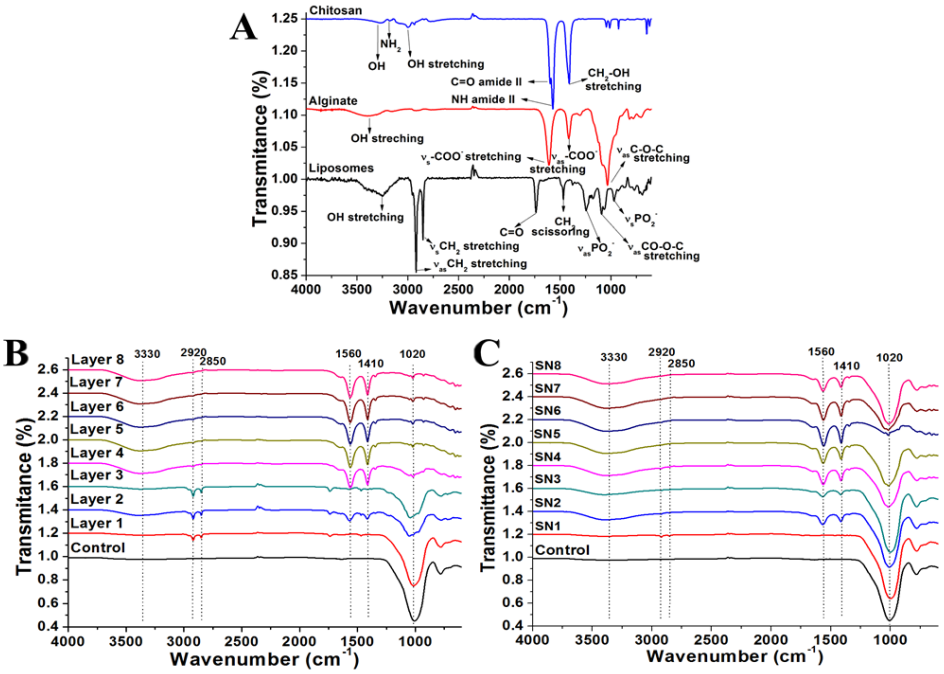

Figure 8. ATR-FTIR spectra of A) chitosan, alginate and liposomes, B) coated liposomal solutions and C) supernatant (SN) obtained after ultracentrifugation of the coated liposomal solutions.

spectrum contains the peaks at 2917, 2850 and 1468 cm^{-1} corresponding to the symmetric, antisymmetric stretching and scissoring mode of CH_2 and a C=O stretching peak at 1737 cm^{-1}, all characteristics of the hydrophobic tail regions of the lipids. Finally, the peaks at 1240 and 1092 cm^{-1} come from the antisymmetric and symmetric stretching modes from PO_2- groups in the hydrophilic head of the lipids.[70-72]

Figure 8 B shows the spectra of the LbL coated liposomes with the titration process described in the materials and methods section. The control is the clean glass substrate with a broad band at 1000 cm^{-1} characteristic of silica glass. On the coated samples, the broad band at 3330 cm^{-1} arise from OH groups in chitosan and alginate signal; the peaks at 2920 and 2850 cm^{-1} arise from the initial liposomes; the peak at 1560 cm^{-1} is the contribution of the NH amide II signal of chitosan overlapped with the COO- stretching of alginate; similarly, the peak at 1410 cm^{-1} is also the contribution of the CH_2-OH and COO- bands of chitosan and alginate, respectively. The small peak that appears at 1020 cm^{-1} corresponds to the C-O-C group of the saccharides.

As the coating process occurs, the characteristic peaks from the liposomes disappear while the characteristic peaks of alginate and chitosan appear, confirming the success of the coating.

Conversely, the FTIR analysis of the supernatant after formation of each PE layer confirmed the presence of none or insignificant amounts of excess unbound PE **(Figure 8 C)**. The small signal of PE along with characteristic peaks of liposomes of layer 1 arise from very small liposomes unable to pellet during the ultracentrifugation step and not due to unadsorbed PE. Although as the coating process advances, the characteristic signals from chitosan and alginate at 1020 cm^{-1} rise in the supernatants, they remain negligible as compared to the signal from the PE layered glass substrate made of the same concentration of PE used during the LbL build up.

4. Conclusions

An aggregation susceptible nanoparticulate drug delivery system, consisting of a soft liposomal core and two weak coating PEs, was successfully prepared using the washless method. The feasibility of adsorption of the weak PEs, alginate and chitosan was first confirmed using QCM, AFM, SEM and EDS studies. The method was later used to assemble 8 saturated layers of coating on the nanoparticle's core. Careful titration curves were produced to ensure the need of no separation steps to remove excess PEs after each layer deposition, as these steps cause irreversible aggregation to this particularly challenging system. The nanoparticles (un-aggregated) were made with almost 100% higher yields and reproducibility as compared to previous attempts to coat the same system using the frequently used method of excesses (5% yield for 6 layer nanoparticles, reproduced twice only).[46, 47] The system's highly biocompatible components together with the ease of controlling its drug release rate and size by tuning the number of layers or performing dilutions, make it a highly desirable candidate for many drug delivery applications. The use of careful titrations can be applied to any aggregation prone nanoparticulate drug delivery system opening doors for experimentation with many more

combinations of coated nanoparticles that have often been avoided because of their weak colloidal stability.

Supporting Information

Supporting Information is available from the Wiley Online Library or from author.

Acknowledgments: The authors acknowledge the financial support of the Natural Science and Engineering Council of Canada (NSERC), the Canadian Institute of Health Research (CIHR) for funding this research and the National Council of Science and Technology of Mexico (CONACYT) for providing F. R. Castiello scholarship. The authors also acknowledge the assistance of Dr. Laila Benameur.

Keywords: Nanoparticle, liposomes, layer by layer self-assembled coating, polyelectrolyte multilayer films, aggregation

[1] A. Akbarzadeh, R. Rezaei-Sadabady, S. Davaran, S. W. Joo, N. Zarghami, Y. Hanifehpour, M. Samiei, M. Kouhi, K. Nejati-Koshki, *Nanoscale Research Letters* **2013**, *8*, 102.
[2] R. A. Schwendener, *Therapeutic Advances in Vaccines* **2014**, *2*, 159.
[3] W. H. De Jong, P. J. A. Borm, *International Journal of Nanomedicine* **2008**, *3*, 133.
[4] G. M. Whitesides, *Nat Biotech* **2003**, *21*, 1161.
[5] P. B. P. J. D. P. P. Biswajit Mukherjee; Niladri Shekhar Dey; Ruma Maji, "Current Status and Future Scope for Nanomaterials in Drug Delivery", in *Application of Nanotechnology in Drug Delivery*, A.D. Sezer, Ed., InTech, 2014.
[6] D. A. LaVan, T. McGuire, R. Langer, *Nat Biotech* **2003**, *21*, 1184.
[7] M. G. Cascone, L. Lazzeri, C. Carmignani, Z. Zhu, *Journal of Materials Science: Materials in Medicine*, *13*, 523.
[8] J. E. Kipp, *International Journal of Pharmaceutics* **2004**, *284*, 109.
[9] A. M. Makhdom, L. Nayef, M. Tabrizian, R. C. Hamdy, *Nanomedicine* **2015**, *11*, 1.
[10] R. Duncan, R. Gaspar, *Molecular Pharmaceutics* **2011**, *8*, 2101.
[11] P. G, *SOJ Pharm Pharm Sci* **2014**, *1*.
[12] T. M. Allen, P. R. Cullis, *Advanced Drug Delivery Reviews* **2013**, *65*, 36.
[13] A. D. S. a. S. B. Melis Çağdaş, "Liposomes as Potential Drug Carrier Systems for Drug Delivery", in *Application of Nanotechnology in Drug Delivery*, A.D. Sezer, Ed., In Tech, 2014.
[14] G. Decher, "Layer-by-Layer Assembly (Putting Molecules to Work)", in *Multilayer Thin Films*, Wiley-VCH Verlag GmbH & Co. KGaA, 2012, p. 1.
[15] X. Qiu, S. Leporatti, E. Donath, H. Möhwald, *Langmuir* **2001**, *17*, 5375.
[16] A. S. H. Makhlouf, "1 - Current and advanced coating technologies for industrial applications", in *Nanocoatings and Ultra-Thin Films*, Woodhead Publishing, 2011, p. 3.

[17] M. M. de Villiers, D. P. Otto, S. J. Strydom, Y. M. Lvov, *Advanced Drug Delivery Reviews* **2011**, *63*, 701.
[18] A. Elbakry, A. Zaky, R. Liebl, R. Rachel, A. Goepferich, M. Breunig, *Nano Letters* **2009**, *9*, 2059.
[19] D. I. Gittins, F. Caruso, *Advanced Materials* **2000**, *12*, 1947.
[20] S. Correa, E. C. Dreaden, L. Gu, P. T. Hammond, *Journal of Controlled Release*.
[21] F. Bordi, S. Sennato, D. Truzzolillo, *Journal of Physics: Condensed Matter* **2009**, *21*, 203102.
[22] V. Mohanta, S. Patil, *Langmuir* **2013**, *29*, 13123.
[23] D. Velegol, P. K. Thwar, *Langmuir* **2001**, *17*, 7687.
[24] Z. S. Haidar, R. C. Hamdy, M. Tabrizian, *Biomaterials* **2008**, *29*, 1207.
[25] G. Bantchev, Z. Lu, Y. Lvov, *J Nanosci Nanotechnol* **2009**, *9*, 396.
[26] A. C. Santos, P. Pattekari, S. Jesus, F. Veiga, Y. Lvov, A. J. Ribeiro, *ACS Applied Materials & Interfaces* **2015**, *7*, 11972.
[27] G. Schneider, G. Decher, *Langmuir* **2008**, *24*, 1778.
[28] T. G. Shutava, S. S. Balkundi, P. Vangala, J. J. Steffan, R. L. Bigelow, J. A. Cardelli, D. P. O'Neal, Y. M. Lvov, *ACS Nano* **2009**, *3*, 1877.
[29] Z. Xiong, H. Qin, H. Wan, G. Huang, Z. Zhang, J. Dong, L. Zhang, W. Zhang, H. Zou, *Chemical Communications* **2013**, *49*, 9284.
[30] E.-C. Wurster, A. Elbakry, A. Göpferich, M. Breunig, "Layer-by-Layer Assembled Gold Nanoparticles for the Delivery of Nucleic Acids", in *Nanotechnology for Nucleic Acid Delivery: Methods and Protocols*, M. Ogris and D. Oupicky, Eds., Humana Press, Totowa, NJ, 2013, p. 171.
[31] G. Schneider, G. Decher, *Nano Letters* **2004**, *4*, 1833.
[32] K. S. Mayya, B. Schoeler, F. Caruso, *Advanced Functional Materials* **2003**, *13*, 183.
[33] Z. Poon, J. B. Lee, S. W. Morton, P. T. Hammond, *Nano Letters* **2011**, *11*, 2096.
[34] K. Fujimoto, T. Toyoda, Y. Fukui, *Macromolecules* **2007**, *40*, 5122.
[35] Y. Fukui, K. Fujimoto, *Langmuir* **2009**, *25*, 10020.
[36] G. B. Sukhorukov, E. Donath, S. Davis, H. Lichtenfeld, F. Caruso, V. I. Popov, H. Möhwald, *Polymers for Advanced Technologies* **1998**, *9*, 759.
[37] F. Caruso, G. Sukhorukov, "Coated Colloids: Preparation, Characterization, Assembly and Utilization", in *Multilayer Thin Films*, Wiley-VCH Verlag GmbH & Co. KGaA, 2003, p. 331.
[38] S. Madrigal-Carballo, S. Lim, G. Rodriguez, A. O. Vila, C. G. Krueger, S. Gunasekaran, J. D. Reed, *Journal of Functional Foods* **2010**, *2*, 99.
[39] D. Guzey, D. J. McClements, *Journal of Agricultural and Food Chemistry* **2007**, *55*, 475.
[40] D. Guzey, D. J. McClements, *J. Agric. Food Chem. Journal of Agricultural and Food Chemistry* **2007**, *55*, 475.
[41] Y. Lvov, P. Pattekari, T. Shutava, *Multilayer Thin Films: Sequential Assembly of Nanocomposite Materials. Edited by Decher G, Schlenoff J. Wiley-VCH* **2012**, 151.
[42] X. Zan, D. A. Hoagland, T. Wang, Z. Su, *Macromolecules* **2012**, *45*, 8805.
[43] L. Zhang, F. X. Gu, J. M. Chan, A. Z. Wang, R. S. Langer, O. C. Farokhzad, *Clinical Pharmacology & Therapeutics* **2008**, *83*, 761.
[44] S. Rodrigues, M. Dion¨ªsio, C. R. n. L¨®pez, A. Grenha, *Journal of Functional Biomaterials* **2012**.
[45] J. Sun, H. Tan, *Materials* **2013**, *6*, 1285.
[46] Z. S. Haidar, *Biomaterials* **2008**, *29*, 1207.
[47] Z. S. Haidar, *Journal of Biomedical Materials Research Part B: Applied Biomaterials* **2009**, *91*, 919.

[48] J. Estelrich, M. Quesada-Perez, J. Forcada, J. Callejas-Fernandez, "CHAPTER 1 Introductory Aspects of Soft Nanoparticles", in *Soft Nanoparticles for Biomedical Applications*, The Royal Society of Chemistry, 2014, p. 1.
[49] M. M. De Villiers, *Advanced Drug Delivery Reviews* **2011**, *63*, 701.
[50] E. Reimhult, M. Zäch, F. Höök, B. Kasemo, *Langmuir* **2006**, *22*, 3313.
[51] A. P. Serro, A. Carapeto, G. Paiva, J. P. S. Farinha, R. Colaço, B. Saramago, *Surface and Interface Analysis* **2012**, *44*, 426.
[52] S. Sennato, F. Bordi, C. Cametti, M. Diociaiuti, P. Malaspina, *Biochimica et Biophysica Acta (BBA) - Biomembranes* **2005**, *1714*, 11.
[53] S. Sennato, F. Bordi, C. Cametti, *The Journal of Chemical Physics* **2004**, *121*, 4936.
[54] J. Araki, *Soft Matter* **2013**, *9*, 4125.
[55] S. Sennato, D. Truzzolillo, F. Bordi, F. Sciortino, C. Cametti, *Colloids and Surfaces A: Physicochemical and Engineering Aspects* **2009**, *343*, 34.
[56] T. Nguyen, A. Grosberg, B. Shklovskii, "Lateral Correlation of Multivalent Counterions is the Universal Mechanism of Charge Inversion", in *Electrostatic Effects in Soft Matter and Biophysics*, C. Holm, P. Kékicheff, and R. Podgornik, Eds., Springer Netherlands, 2001, p. 469.
[57] S.-J. Lim, C.-K. Kim, *International Journal of Pharmaceutics* **2002**, *243*, 135.
[58] S. A. Wissing, R. H. Müller, *Journal of Controlled Release* **2002**, *81*, 225.
[59] P. Ahlin, J. Kristl, A. Kristl, F. Vrečer, *International Journal of Pharmaceutics* **2002**, *239*, 113.
[60] H. Wang, O. C. Boerman, K. Sariibrahimoglu, Y. Li, J. A. Jansen, S. C. G. Leeuwenburgh, *Biomaterials* **2012**, *33*, 8695.
[61] G. Kong, R. D. Braun, M. W. Dewhirst, *Cancer Research* **2000**, *60*, 4440.
[62] M. Salomäki, I. A. Vinokurov, J. Kankare, *Langmuir* **2005**, *21*, 11232.
[63] H. L. Tan, M. J. McMurdo, G. Pan, P. G. Van Patten, *Langmuir* **2003**, *19*, 9311.
[64] M. Salomäki, P. Tervasmäki, S. Areva, J. Kankare, *Langmuir* **2004**, *20*, 3679.
[65] B. Schwarz, M. Schönhoff, *Langmuir* **2002**, *18*, 2964.
[66] J. E. Wong, F. Rehfeldt, P. Hänni, M. Tanaka, R. v. Klitzing, *Macromolecules* **2004**, *37*, 7285.
[67] R. v. Klitzing, *Physical Chemistry Chemical Physics* **2006**, *8*, 5012.
[68] J. de Grooth, R. Oborný, J. Potreck, K. Nijmeijer, W. M. de Vos, *Journal of Membrane Science* **2015**, *475*, 311.
[69] M. A. A. Shafie, H. H. M. Fayek, *Journal of Clinical & Experimental Ophthalmology* **2013**, *2013*.
[70] J. Hanlan, D. A. Skoog, D. M. West, "Principles of Instrumental Analysis", JSTOR, 1973.
[71] I. A. Mudunkotuwa, *Analyst* **2014**, *139*, 870.
[72] R. Tantipolphan, *International Journal of Pharmaceutics* **2007**, *337*, 40.

.

Click here to access/download

Production Data

Production Data.zip